Mechanical properties of LaCoO$_3$ based ceramics

Nina Orlovskaya, Kjersti Kleveland, Tor Grande, Mari-Ann Einarsrud*

Department of Inorganic Chemistry, Norwegian University of Science and Technology, 7034 Trondheim, Norway

Abstract

Mechanical characteristics of LaCoO$_3$ based ceramics have been measured over the temperature range from room temperature (RT) to 850°C. The bending strength is in the range of 53 MPa for 83% dense LaCoO$_3$, 76 MPa for 90% dense La$_{0.8}$Sr$_{0.2}$CoO$_3$, and 150 MPa for 99% dense La$_{0.8}$Ca$_{0.2}$CoO$_3$ ceramics at RT. The strength of LaCoO$_3$ and La$_{0.8}$Sr$_{0.2}$CoO$_3$ was relatively independent of temperature up to 850°C. The strength of the dense La$_{0.8}$Ca$_{0.2}$CoO$_3$ material decreased linearly to 850°C, where the strength at 850°C is only about 50% of the strength at RT. The fracture mode of this material is changed from fully transgranular at RT to mixed trans- and intergranular at 850°C. Hardness in the range of 7–9 GPa for 90% dense La$_{0.8}$Sr$_{0.2}$CoO$_3$ and 9–11 GPa for fully dense La$_{0.8}$Ca$_{0.2}$CoO$_3$ ceramics have been observed. The fracture toughness is calculated to be 0.73 ± 0.08 MPa m$^{1/2}$ for 90% dense La$_{0.8}$Sr$_{0.2}$CoO$_3$, and 0.98 ± 0.09 MPa m$^{1/2}$ for fully dense La$_{0.8}$Ca$_{0.2}$CoO$_3$ ceramics. Young's modulus for dense La$_{0.8}$Ca$_{0.2}$CoO$_3$ was measured to be 112 ± 3 GPa. © 1999 Published by Elsevier Science Ltd. All rights reserved.

Keywords: LaCoO$_3$; Hardness; Mechanical properties; Strength; Toughness

1. Introduction

In recent years there has been considerable interest in perovskite oxides for application in solid oxide fuel cells (SOFC), exhaust gas sensors in automobiles, membranes for separation processes and as catalysts.[1] Important requirements for the materials for the above applications in addition to high electronic and/or ionic conductivity are stability in the temperature range and the environment of operation, as well as satisfactory mechanical properties. LaCoO$_3$ based materials are interesting for these applications due to their high electronic and ionic conductivity when La is substituted by divalent cations. LaCoO$_3$ has a perovskite-type structure with La on A-site and Co on B-site, and the oxygen stoichiometry varies with O$_2$ pressure and temperature. Substituting on the A-site of LaCoO$_3$ with either Sr or Ca increases the oxygen deficiency and hence increases particularly the ionic conductivity. No first order transition of pure LaCoO$_3$ has been reported. The rhombohedral distortion from cubic symmetry is linearly decreasing with increasing temperature.[2] A second order

like transition related to a semiconductor to metallic "like" transition is reported at 450–650 K.[3] Sr-substituted LaCoO$_3$ becomes cubic at about 50 at% Sr.[4] The semiconductor to metallic transition temperature is decreasing with increasing Sr content.[4] A similar effect of Ca-substitution up to 20 at% has been reported by Sehlin et al.[5]

Other properties of LaCoO$_3$ based materials such as oxygen non-stoichiometry, catalytic behavior, stability and diffusion are also fairly well described.[6–9] Comparatively little research has been carried out on the mechanical properties of LaCoO$_3$ based ceramics. However, for the industrial applications of LaCoO$_3$ based materials, i.e. as oxygen separating membranes operating at 800–1000°C, knowledge of mechanical properties is necessary. The aim of the present study was therefore to prepare LaCoO$_3$, La$_{0.8}$Sr$_{0.2}$CoO$_3$ and La$_{0.8}$Ca$_{0.2}$CoO$_3$ ceramics and to measure the mechanical properties such as bending strength, hardness, fracture toughness and Young's modulus at RT and at temperatures to 850°C.

2. Experimental procedure

Powders with expected stoichiometry LaCoO$_3$, La$_{0.8}$Sr$_{0.2}$CoO$_3$ and La$_{0.8}$Ca$_{0.2}$CoO$_3$ were prepared by a

---

* Corresponding author. Tel.: + 47-73-594002; fax: + 47-73-590860.
E-mail address: mari-ann.einarsrud@chembio.ntnu.no (M.-A. Einarsrud).

Table 1
Chemical composition, density, porosity, average grain size and secondary phases present in the densified ceramics

Sample code	Sample composition	Density (g/cm³)	Porosity[a] (%)	Grain size (μm)	Secondary phases
$LaCoO_3$	$La_{1.077}CoO_3$	6.077 ± 0.02	16.6	2–3	La_2O_3
$La_{0.8}Ca_{0.2}CoO_3$	$La_{0.922}Ca_{0.221}CoO_3$	6.695 ± 0.03	0.15	1–2	CaO–CoO
$La_{0.8}Sr_{0.2}CoO_3$	$La_{0.878}Sr_{0.199}CoO_3$	6.274 ± 0.005	9.5	2–3	$La_{2-x}Sr_xCoO_4$

[a] Calculated from the theoretical densities of the pure compounds without secondary phases.

wet chemical route using ethylenediamine tetra acetate acid (EDTA) as a complexing agent. The cations were provided from nitrate solutions and the gel formation took place at 80°C in the solution with adjusted pH (10 for La and Co and 7 when Ca and Sr were present). The concentration of the nitrate solutions used during synthesis and the stoichiometry of the synthesized powders were measured by an Atom Scan 16 ICP-AES Spectrometer (Thermo Jarrell Ash Corp.). After drying and removal of organic residue at 600°C, the powders were ball milled with Si_3N_4 balls and calcined at 850°C ($La_{0.8}Ca_{0.2}CoO_3$) or 900°C ($LaCoO_3$, $La_{0.8}Sr_{0.2}CoO_3$) for 24 h in flowing air. After calcination, the powders were further dry ball milled for 3 h and pressed into bars ($7 \times 10 \times 55$ mm³) at uniaxial pressure of 30 MPa followed by cold isostatic pressing at 300 MPa. The bars were sintered at 1200°C for 3 h in a powder bed of $LaCoO_3$. The heating and cooling rate was set to 300 K/h and a dwell time of 2 h at 500°C during heating was included in the sintering program. The real heating rate might have been lower than the set value due to the insulating effect of the powder bed.

The bulk density of the ceramics was measured by the liquid immersion method using isopropanol. Powder X-ray diffraction (XRD) of the powders and ground ceramics was performed on a Siemens D5005 diffractometer with Cu K_α-radiation and a secondary monochromator. Microstructure of the samples was studied by SEM (Zeiss DSM 940). Grain size was measured from SEM micrographs of polished and thermally etched surfaces. After polishing to 1 μm diamonds, Vickers hardness was measured at loads up to 500 g (Digital Micro Hardness tester MX T70, Matsuzawa). Fracture toughness of $La_{0.8}Sr_{0.2}CoO_3$ and $La_{0.8}Ca_{0.2}$-CoO_3 was calculated after indentation tests at 300 g force, when cracks appeared at the impression corners.[10] Four-point bending strength of the machined (Mil STD 1942B) specimens was determined at RT, 650 and 850°C using an inner span of 20 mm and an outer span of 40 mm and a heating rate of 15–25 K/min. Specimen dimensions were approximately $4 \times 5.5 \times 43$ mm³ and normally 4 to 5 bars were tested for each composition and temperature. Young's modulus was determined at room temperature by measuring the deflection of samples during 4-point bending tests

according to the ASTM 855-90 standard. All the measurements were performed in air.

3. Results and discussion

3.1. Characterization of LaCoO₃ based ceramics

The chemical analysis of the calcined powders included in Table 1 showed a deviation in the stoichiometry from the expected value due to an error introduced during the standardization of the nitrate solutions. For simplicity we will hereafter refer to the samples as $LaCoO_3$, $La_{0.8}Sr_{0.2}CoO_3$ and $La_{0.8}Ca_{0.2}CoO_3$ despite the known non-stoichiometry. The grain size of all the three powders was in the same range (0.2–0.5 μm) after calcination and all the three powders appeared single phase by XRD. From XRD patterns, the Sr-substituted sintered ceramics contained some $La_{2-x}Sr_xCoO_4$ as secondary phase, the Ca-substituted ceramics contained small amounts of CaO–CoO(ss) secondary phase while La_2O_3 was observed in $LaCoO_3$. The density of the
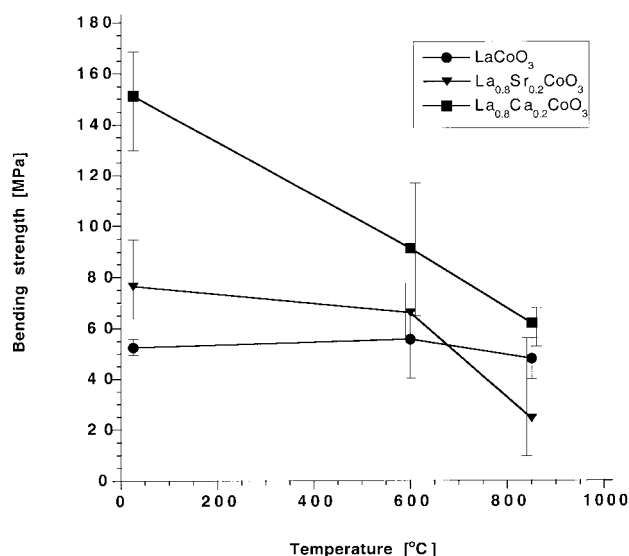

Fig. 1. Bending strength of $LaCoO_3$, $La_{0.8}Sr_{0.2}CoO_3$ and $La_{0.8}Ca_{0.2}$-CoO_3 ceramics as a function of temperature. The error bars shows the maximum and minimum in strength obtained for each composition and temperature.

ceramics after sintering at 1200°C for 3 h as well as the average grain size of materials are included in Table 1.

3.2. Strength

The bending strength of the three different materials as a function of temperature is shown in Fig. 1. Dense $La_{0.8}Ca_{0.2}CoO_3$ has a bending strength of 150 MPa whereas the more porous $La_{0.8}Sr_{0.2}CoO_3$ and $LaCoO_3$ have lower values of 76 and 53 MPa, respectively. Balachandran et al.[11] reported a flexural strength of 120.4 ± 6.8 MPa for a sample with 7% porosity and stoichiometry close to $La_{0.25}Sr_{0.8}Fe_{0.6}Co_{0.4}O_x$, which is comparable to our strength data. For $LaCoO_3$ and $La_{0.8}Sr_{0.2}CoO_3$ which are both quite porous, the strength shows only a small decrease with increasing temperature up to 850°C. However, a linear decrease in bending strength to about 50% was observed for $La_{0.8}Ca_{0.2}CoO_3$ when increasing the temperature to 850°C. The fracture surface of $La_{0.8}Ca_{0.2}CoO_3$ ceramics shows a transgranular fracture mode at RT [Fig. 2(a)],

while at high temperature the character of the fracture changes and both inter- and transgranular fracture exist [Fig. 2(b) and (c)]. In the two porous samples ($LaCoO_3$ and $La_{0.8}Sr_{0.2}CoO_3$), both inter- and transgranular fracture modes were observed independent of temperature. The observed decrease in strength for $La_{0.8}Ca_{0.2}CoO_3$ with increasing temperature is probably due to a reaction between the perovskite and secondary CaO–CoO(ss) (Table 2) during the reheating of the samples during testing. $La_{0.8}Ca_{0.2}CoO_3$ and CaO are not co-existing phases below 1026°C.[12,13] The formation of a secondary phase was observed on some parts of the fracture surface after high temperature testing and this phase is most probably $Ca_3Co_2O_6$ which is a stable phase in the CaO–CoO system in air.[13] Interfacial segregation to the grain boundaries might be another reason for the observed decrease in strength and change in fracture mode for $La_{0.8}Ca_{0.2}CoO_3$.[14] Fracture origin in most of the samples were large pores (voids) (20 to 200 μm) located near the surface of the specimens or large grains of secondary phases, i.e. CaO for Ca-substituted material

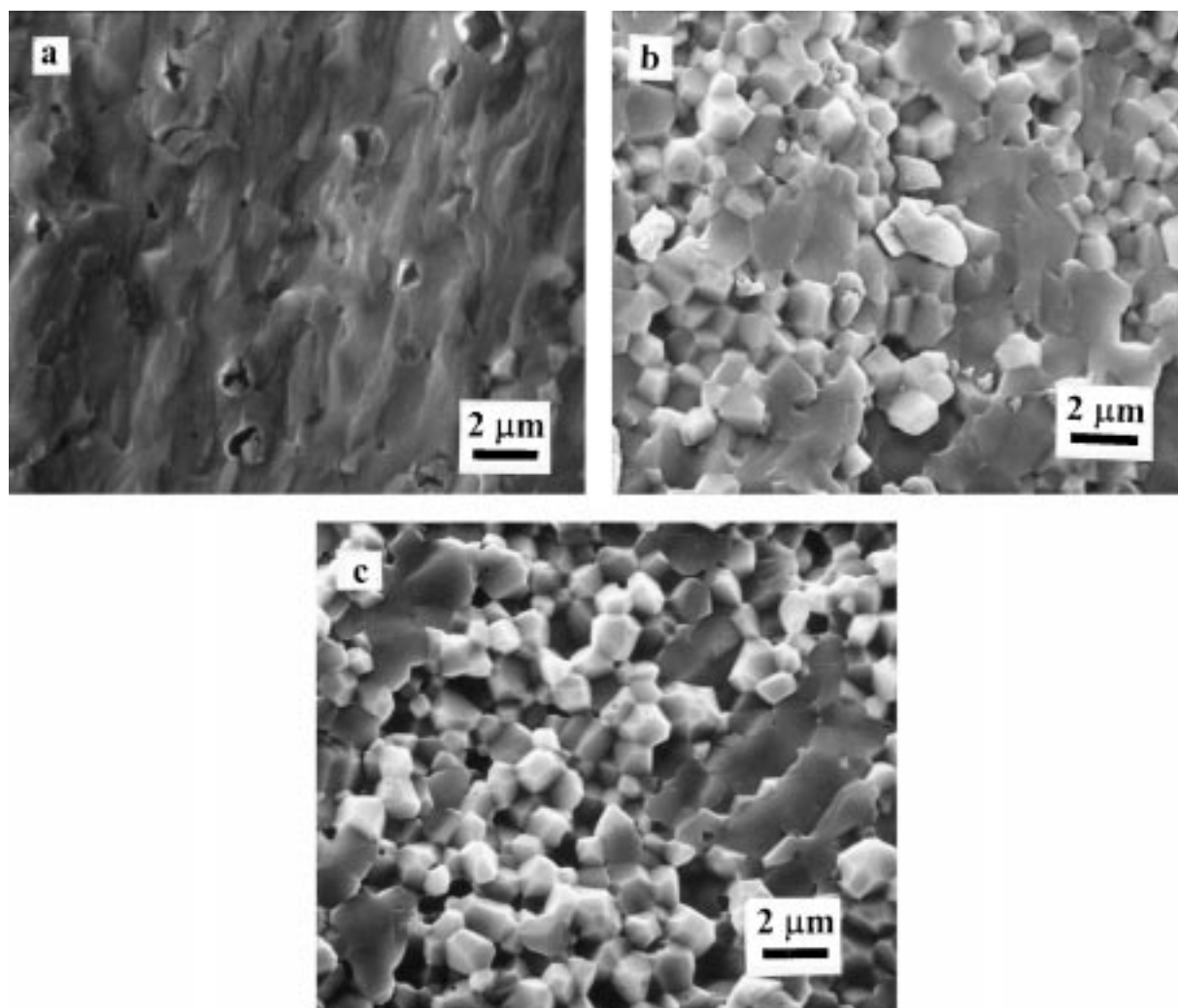Fig. 2. Fracture surfaces of $La_{0.8}Ca_{0.2}CoO_3$ ceramics at (a) RT; (b) 600°C and (c) 850°C.

(Fig. 3). The large pores were originating from the green body preparation. A decrease in strength is also observed for phase pure La based chromites heated above 500°C by Mori et al.[15] and Montross et al.[16] The knowledge of the noticeable decrease in strength at temperatures interesting for applications is important, i.e. for the design of membranes for oxygen separation.

3.3. Hardness and fracture toughness

The hardness as function of applied load for $La_{0.8}Sr_{0.2}CoO_3$ and $La_{0.8}Ca_{0.2}CoO_3$ ceramics is shown in Fig. 4. Some softening effect can be seen for the hardness values at low loads for $La_{0.8}Sr_{0.2}CoO_3$. However, due to high scattering of hardness data at low load, it is difficult to obtain the exact number. It should be noticed that the hardness value is dependent on the porosity of the materials,[17] and is equal to 7–9 GPa for $La_{0.8}Sr_{0.2}CoO_3$ with 10% porosity and 9–11 GPa for dense $La_{0.8}Ca_{0.2}CoO_3$ material. The first cracks after indentation appeared at 300 g loading which is an indirect indication of the very brittle nature of $LaCoO_3$ based ceramics. The fracture toughness for $La_{0.8}Sr_{0.2}CoO_3$ and $La_{0.8}Ca_{0.2}CoO_3$ was calculated from inden-

tation measurement.[10] A value of 0.73 ± 0.08 MPa m$^{1/2}$ was obtained for $La_{0.8}Sr_{0.2}CoO_3$ and 0.98 ± 0.09 MPa m$^{1/2}$ for $La_{0.8}Ca_{0.2}CoO_3$ which is in good agreement with the fracture toughness of $BaTiO_3$ of 1.0 MPa m$^{1/2}$.[18] The typical Vickers impression of $La_{0.8}Sr_{0.2}CoO_3$ ceramics is shown in Fig. 5. As can be seen, the ratio $c/a > 2.0$, where c is the crack length and a is the indentation half diagonal, suggesting that the type of cracks after indentation is a median or a half-penny type.

3.4. Young's modulus

The Young's moduli of the tested specimens are shown in Table 2 which also includes calculated Young's moduli of 100% dense samples assuming the same relative E-modulus to porosity behavior of these samples as $CaTiO_3$ ceramics previously reported in the literature.[19] This relative Young's modulus to porosity behavior fits well with a theoretical model published by Boccaccini and Fan,[20] where a porous material can be treated as a special case of a two-phase composite with the Young's modulus of one phase (pore) is equal to zero. The Young's moduli of 100% dense samples calculated using the model presented by Selcuk and

Table 2
The measured E-modulus of the tested specimens at room temperature and the E-modulus calculated for 100% dense materials using the theory of Boccacini and Fan[16] and Seluk and Atkinson[17]

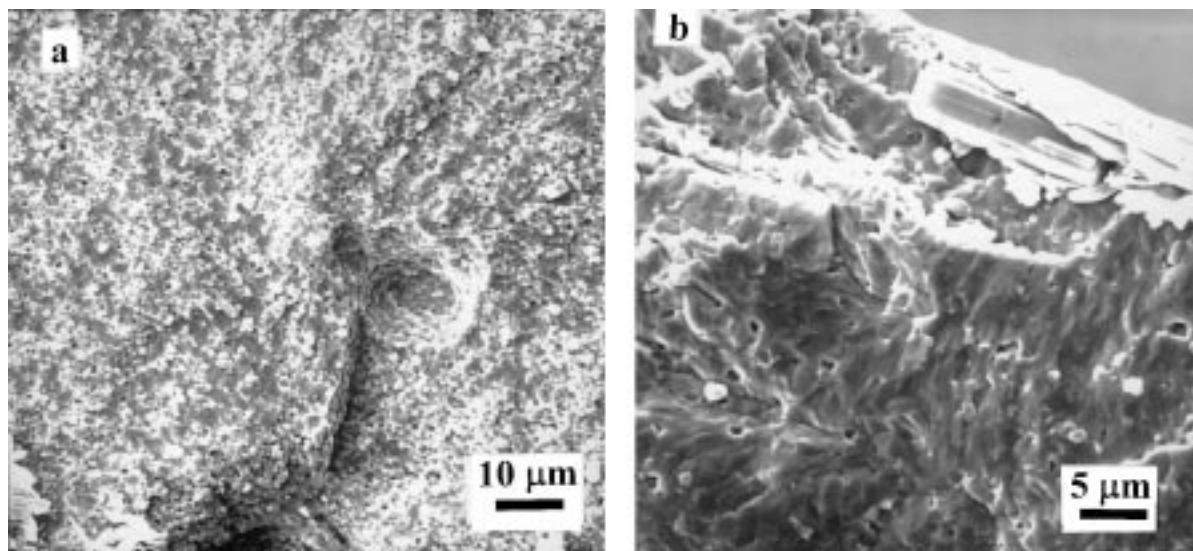| Composition	Measured Young's modulus (GPa)	Estimated Young's modulus 100% density[16] (Gpa)	Estimated Young's modulus 100% density[17] (GPa)
$LaCoO_3$	47.8 ± 7.8	78 ± 3	83 ± 3
$La_{0.8}Ca_{0.2}CoO_3$	111.5 ± 2.8	112 ± 3	112 ± 3
$La_{0.8}Sr_{0.2}CoO_3$	64.4 ± 9.4	87 ± 13	86 ± 13

Fig. 3. Fracture origins of $La_{0.8}Ca_{0.2}CoO_3$ ceramics: (a) void and (b) CaO crystal.

Atkinson[21] assuming a Poisson's ratio of 0.3 is also given in Table 2. There is an excellent fit between the two methods for calculating Young's moduli for dense samples. To our knowledge these are the first published Young's modulus data for $LaCoO_3$-based ceramics. However, Balachandran et al.[12] have reported a Young's modulus of 124 ± 3 GPa for a sample with
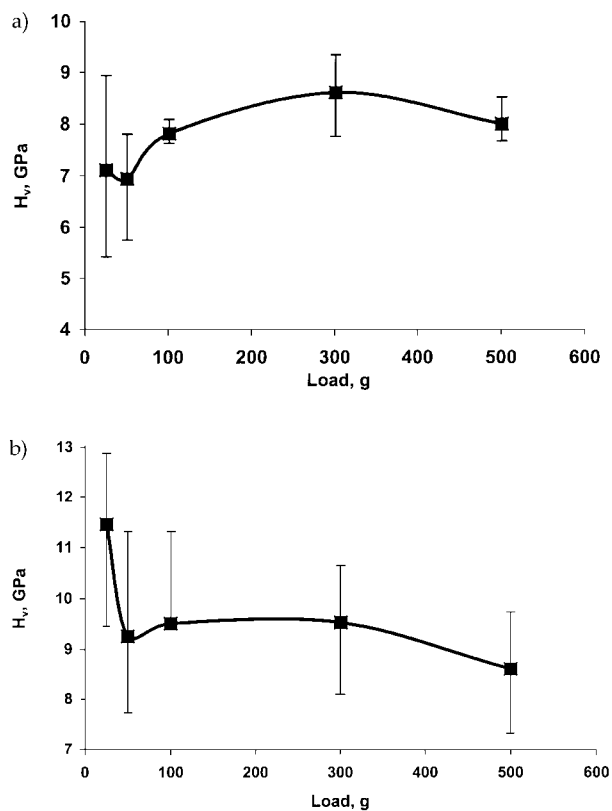
Fig. 4. Hardness of (a) $La_{0.8}Sr_{0.2}CoO_3$ and (b) $La_{0.8}Ca_{0.2}CoO_3$ ceramics as a function of load.
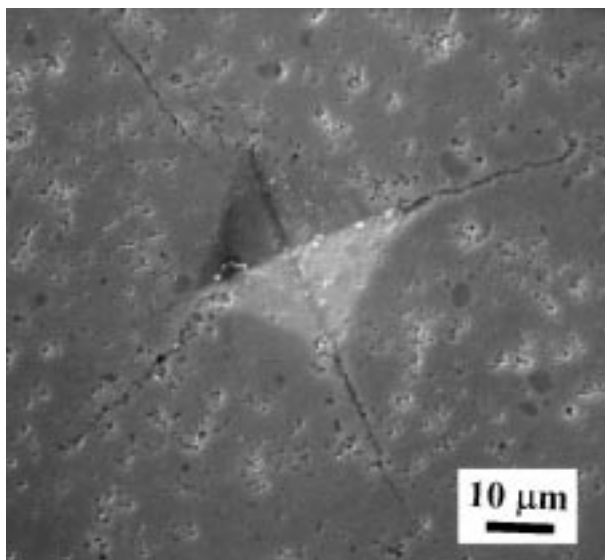
Fig. 5. Vickers impression on $La_{0.8}Sr_{0.2}CoO_3$ ceramics.

stoichiometry close to $La_{0.2}Sr_{0.8}Fe_{0.6}Co_{0.4}O_x$. Cheng et al.[22] have recently published the modulus of elasticity of $BaTiO_3$ as a function of temperature and structure. Our data for the $LaCoO_3$-based materials are in the same range as the E-modulus for $BaTiO_3$. However, it seems that the calculated values for the porous materials are somewhat underestimated. This underestimation might be due to a non-linear stress–strain behavior observed for these materials (Orlovskaya, Einarsrud, Gogotsi, Gogotsi, Grande and Moe, unpublished results) and hence the approximations used in the estimations are not completely valid. The Ca-substituted sample shows a higher Young's modulus value than the other two samples. Sr-doping of $LaCoO_3$ has been shown to reduce the rhombohedral distortion with increasing amount of Sr doping up to $La_{0.45}Sr_{0.55}CoO_3$ for which the structure becomes cubic.[4] For $BaTiO_3$ there is an increase in Young's modulus with increase in symmetry of the crystal system interrupted by a decrease close to the phase transition temperature.[22] The explanation for the increased Young's modulus for especially the Ca-substituted sample might therefore be a reduced distortion of the crystal symmetry compared to $LaCoO_3$. Also, an increase in Young's modulus is expected with increasing oxidation state of Co. Other factors like grain size[20] might also influence the Young's moduli, however, in our study the grain size of the samples was quite similar.

4. Conclusions

The bending strength is in the range of 53 MPa for 83% dense $LaCoO_3$, 76 MPa for 90% dense $La_{0.8}Sr_{0.2}CoO_3$, and 151 MPa for fully dense $La_{0.8}Ca_{0.2}CoO_3$ ceramics. For $LaCoO_3$ and $La_{0.8}Sr_{0.2}CoO_3$, the strength shows only a small decrease with increasing temperature up to 850°C. The strength of the dense $La_{0.8}Ca_{0.2}CoO_3$ ceramics linearly decreased to only approximately 50% of the strength at RT. For $La_{0.8}Ca_{0.2}CoO_3$ ceramics the fracture mode changes from fully transgranular for fracture at RT to mixed trans- and intergranular fracture after high temperature testing. Vickers microhardness is in the range of 7–9 GPa for 90% dense $La_{0.8}Sr_{0.2}CoO_3$, and 9–11 GPa for fully dense $La_{0.8}Ca_{0.2}CoO_3$ ceramics. The fracture toughness is calculated to be 0.73 ± 0.08 MPa m$^{1/2}$ for 90% dense $La_{0.8}Sr_{0.2}CoO_3$, and 0.98 ± 0.09 MPa m$^{1/2}$ for fully dense $La_{0.8}Ca_{0.2}CoO_3$ ceramics. Young's modulus for dense $La_{0.8}Ca_{0.2}CoO_3$ was measured to be 112 ± 3 GPa.

Acknowledgements

References

1. Alcock, C. B., Doshi, K. D. and Shen, Y., Perovskite electrodes for sensors. *Solid State Ionics*, 1992, **51**, 281–289.
2. Raccah, P. M. and Goodenough, J. B., First order localized-electron collective-electron transition in $LaCoO_3$. *Phys. Rev.*, 1967, **155**, 932.
3. Stølen, S., Grønvold, F. and Brinks, H., Energetics of the spin transition in $LaCoO_3$. *Phys. Rev. B*, 1997, **55**, 14103–14106.
4. Mineshige, A., Inaba, M., Yao, T. and Ogumi, Z., Crystal structure and metal–insulator transition of $La_{1-x}Sr_x$-CoO_3. *J. Solid State Chem.*, 1996, **121**, 423–429.
5. Sehlin, S. R., Anderson, H. U. and Sparlin, D. M., Semiempirical model for the electrical properties of $La_{1-x}Ca_x$-CoO_3. *Phys. Rev. B*, 1995, **52**, 11681–11689.
6. Mizusaki, J., Mima, Y., Yamauchi, S., Fueki, K. and Tagawa, H., Nonstoichiometry of the perovskite-type oxides $La_{1-x}Sr_xCoO_{3-\delta}$. *J. Solid State Chem.*, 1989, **80**, 102–111.
7. Islam, M. S., Cherry, M. and Winch, L. J., Defect chemistry of $LaBO_3$ (B = Al, Mn or Co) perovskite-type oxides. *J. Chem. Soc. Faraday Trans.*, 1996, **92**, 479–482.
8. Mizusaki, J., Nonstoichiometry, diffusion and electrical properties of perovskite-type oxide electrode materials. *Solid State Ionics*, 1992, **52**, 79–91.
9. Ohno, Y., Nagata, S. and Sato, N., Properties of oxides for high temperature solid electrolyte fuel cell. *Solid State Ionics*, 1983, **9/10**, 1001–1008.
10. Antis, G. R., Chantikul, P., Lawn, B. R. and Marshall, D. B., A critical evaluation of indentation techniques for measuring fracture toughness: I. Direct crack measurements. *J. Am. Ceram. Soc.*, 1981, **64**, 533–538.
11. Balachandran, U., Dusek, J. T., Sweeney, S. M., Poeppel, R. B., Mieville, R. L., Maiya, P. S., Kleefisch, M. S., Pei, S., Kobylinski, T. P., Udovich, C. A. and Bose, A. C., Methane to syngas via ceramic membranes. *Am. Ceram. Soc. Bull.*, 1995, **74**, 71–75.
12. Kleveland, K., Einarsrud, M.-A. and Grande, T., Sintering of $LaCoO_3$ based ceramics. *J. Eur. Ceram. Soc.*, in press.
13. Levin, E. M., Robbins, C. R. and McMurdie, H. F., Phase Diagrams for Ceramists. *Am. Ceram. Soc.*, 1964.
14. Desu, S. and Payne, D., Interfacial segregation in perovskites: I. theory; II. experimental evidence. *J. Am. Ceram. Soc.*, 1990, **73**(11), 3391–3406.
15. Mori, M., Itoh, H., Mori, N. and Abe, T., Mechanical, electrical properties of alkaline earth metal doped lanthanum chromites. In *Proceedings of the 3rd International Symposium on Solid Oxide Fuel Cells*, ed. S. C. Sinhal and H. Iwahara. Electrochem. Soc, Tokyo, Japan, 1993, pp. 325–334.
16. Montross, C. S., Yokokawa, H., Dokiya, M. and Bekessy, L., Mechanical properties of magnesia-doped lanthanum chromite versus temperature. *J. Am. Ceram. Soc.*, 1995, **78**, 1869–1872.
17. McColm, I. J., *Ceramic Hardness*. Plenum Press, New York, 1990.
18. Blamey, J. M. and Parry, T. V., The effect of processing variables on the mechanical and electrical properties of barium titanate positive-temperature-coefficient-of-resistance ceramics. *J. Mater. Sci.*, 1993, **28**, 4317–4324.
19. Jauch, U., Zur Thermoschockbest-ndigkeit mehrphasiger Werkstoffe. *Ber. KfK Karlsruhe*, 1989, 4469.
20. Boccacchini, A. R. and Fan, Z., A new approach for the Young's modulus–porosity correlation of ceramic materials. *Ceramics Int.*, 1997, **23**, 239–245.
21. Selcuk, A. and Atkinson, A., Elastic properties of ceramic oxides used in solid oxide fuel cells (SOFC). *J. Eur. Ceram. Soc.*, 1997, **17**, 1523–1532.
22. Cheng, B. L., Gabbay, M., Duffy, W. Jr. and Fantozzi, G., Mechanical loss and Young's modulus associated with phase transitions in barium titanate based ceramics. *J. Mater. Sci.*, 1996, **31**, 4951–4955.